Biology of Reproduction, 2022, 1–13
https://doi.org/10.1093/biolre/ioac209
Research Article

SWI/SNF chromatin remodeling subunit *Smarca4*/BRG1 is essential for female fertility†

Atefeh Abedini[1,2,‡], David A. Landry[1,2,3,*,‡], Angus D. Macaulay[4], Het Vaishnev[1,2], Ashna Parbhakar[2], Dalia Ibrahim[1,2], Reza Salehi[4], Vincent Maranda[1,2], Elizabeth Macdonald[1,2] and Barbara C. Vanderhyden[1,2,*]

[1]Department of Cellular and Molecular Medicine, University of Ottawa, Ottawa, ON, Canada
[2]Cancer Therapeutics Program, Ottawa Hospital Research Institute, Ottawa, ON, Canada
[3]Interdisciplinary School of Health Sciences, University of Ottawa, Ottawa, ON, Canada
[4]Chronic Diseases Program, Ottawa Hospital Research Institute, Ottawa, ON, Canada
***Correspondence:** Cancer Therapeutics Program, Ottawa Hospital Research Institute, 501 Smyth Road, Box 926, Ottawa, ON K1H 8L6, Canada.
E-mail: dlandry5@uottawa.ca (David A. Landry) or E-mail: bvanderhyden@ohri.ca (Barbara C. Vanderhyden)

†**Grant Support:** This work was supported by grants from the Canadian Rare Disease Models and Mechanisms Network and the Cancer Research Society. D.A.L was supported by postdoctoral fellowships from the Natural Sciences and Engineering Research Council of Canada (NSERC) and the Lalor Foundation. A.A. was supported by a fellowship from the Lalor Foundation.

‡These authors contributed equally: Atefeh Abedini and David A. Landry.

Abstract

Mammalian folliculogenesis is a complex process that involves the regulation of chromatin structure for gene expression and oocyte meiotic resumption. The SWI/SNF complex is a chromatin remodeler using either Brahma-regulated gene 1 (BRG1) or BRM (encoded by *Smarca4* and *Smarca2*, respectively) as its catalytic subunit. SMARCA4 loss of expression is associated with a rare type of ovarian cancer; however, its function during folliculogenesis remains poorly understood. In this study, we describe the phenotype of BRG1 mutant mice to better understand its role in female fertility. Although no tumor emerged from BRG1 mutant mice, conditional depletion of *Brg1* in the granulosa cells (GCs) of *Brg1$^{fl/fl}$;Amhr2-Cre* mice caused sterility, whereas conditional depletion of *Brg1* in the oocytes of *Brg1$^{fl/fl}$;Gdf9-Cre* mice resulted in subfertility. Recovery of cumulus-oocyte complexes after natural mating or superovulation showed no significant difference in the *Brg1$^{fl/fl}$;Amhr2-Cre* mutant mice and significantly fewer oocytes in the *Brg1$^{fl/fl}$;Gdf9-Cre* mutant mice compared with controls, which may account for the subfertility. Interestingly, the evaluation of oocyte developmental competence by in vitro culture of retrieved two-cell embryos indicated that oocytes originating from the *Brg1$^{fl/fl}$;Amhr2-Cre* mice did not reach the blastocyst stage and had higher rates of mitotic defects, including micronuclei. Together, these results indicate that BRG1 plays an important role in female fertility by regulating granulosa and oocyte functions during follicle growth and is needed for the acquisition of oocyte developmental competence.

Summary Sentence

Conditional depletion of Brahma-regulated gene 1 in granulosa cells early in follicle development and in oocytes results in sterile and subfertile phenotypes, respectively.

Received: November 10, 2022. **Revised:** July 21, 2022. **Accepted:** November 22, 2022

Graphical Abstract

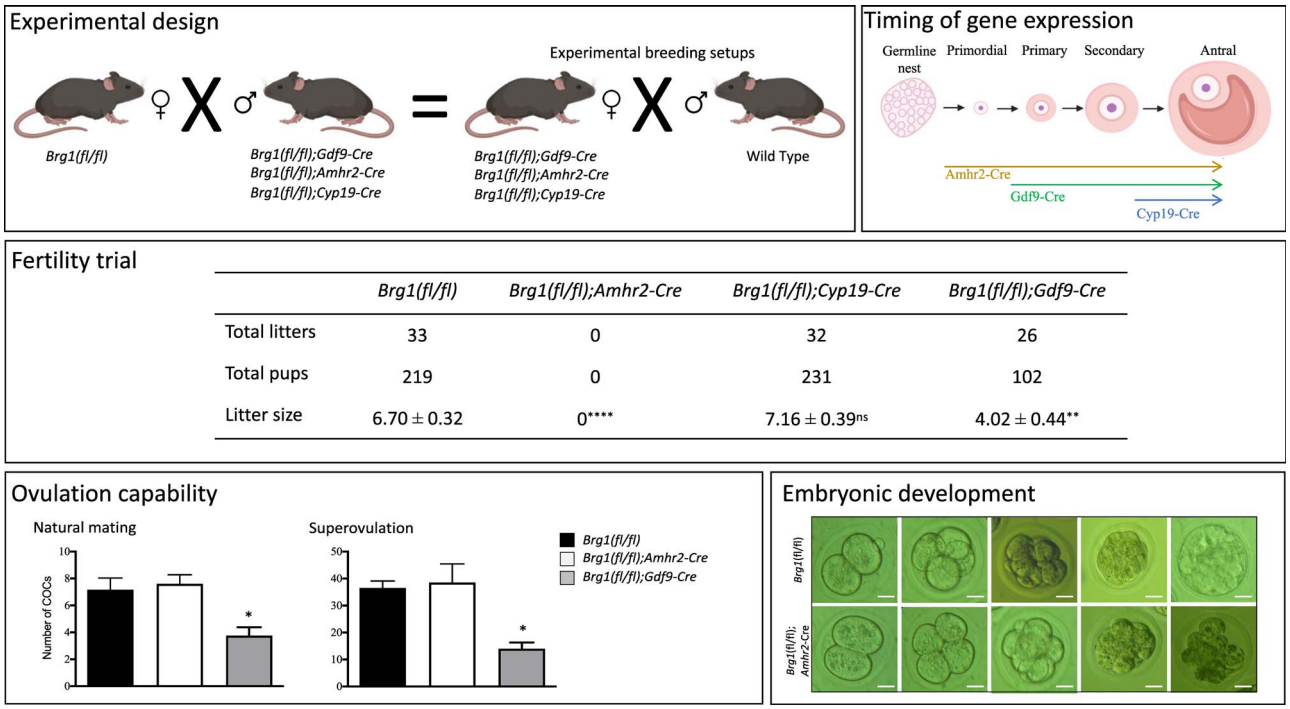

	Brg1(fl/fl)	Brg1(fl/fl);Amhr2-Cre	Brg1(fl/fl);Cyp19-Cre	Brg1(fl/fl);Gdf9-Cre
Total litters	33	0	32	26
Total pups	219	0	231	102
Litter size	6.70 ± 0.32	0****	7.16 ± 0.39^{ns}	4.02 ± 0.44**

Keywords: oocyte, granulosa cells, SWI/SNF complex, infertility, oocyte quality, embryos

Introduction

Oocyte developmental competence is acquired during folliculogenesis and is strongly associated with the follicle status [1]. The process of folliculogenesis consists of the activation and progression of primordial follicles through several stages to become large preovulatory follicles capable of ovulation. Communication among the different cell types within the follicle is critical for coordinated proliferation and proper differentiation. The period of time between the exponential growth under FSH and the LH surge is known as a critical period for oocyte developmental competence acquisition and is referred to as follicle capacitation [2, 3]. During that period, granulosa cells (GCs) modify their gene expression to prepare the molecular machinery for the LH surge and confer the oocyte with the capacity for molecular maturation [1]. Throughout folliculogenesis, the oocyte stockpiles mRNAs, known as maternal mRNAs, that are essential for its first few cell divisions after fertilization and the zygotic genome activation (ZGA) at the two-cell stage in mice [4]. The ZGA is a nuclear reprogramming event that transitions the newly formed genome from transcriptional quiescence to a highly transcriptional state. We have previously shown that SWI/SNF-related (SWItch/Sucrose Non-Fermentable) chromatin remodeling complexes regulate the follicular gene expression associated with acquisition of oocyte developmental competence [5–7]. Moreover, a member of the SWI/SNF complex, Brahma-regulated gene 1 (BRG1; encoded by *Smarca4*), was the first gene reported to be required for the ZGA in mouse oocytes [8].

Smarca4 (BRG1) and *Smarca2* (Brahma, BRM) encode for the two possible catalytic subunits of the SWI/SNF complex that uses the energy of ATP hydrolysis to modify chromatin structure to regulate the transcription of genes repressed by chromatin [9]. All SWI/SNF complexes contain one catalytic core, either BRG1 or BRM, which are important ATPase subunits of the complex that modulates transcription to regulate the biological function of the cells. Genetic information is stored within the chromatin, formed from repeated nucleosomes (DNA and histone proteins H1, H2A, H2B, H3, and H4) that are modulated to control DNA replication, repair, and gene expression by histone-modifying enzymes and ATP-dependent chromatin remodeling proteins such as the SWI/SNF complex. Some histones, such as histone H3, play crucial regulatory roles during folliculogenesis [10]; their modification is correlated with the transcriptional activity necessary for cellular division [11] and links to FSH and estradiol action during the preovulatory period [12]. Those data suggest a direct role of H3 modulation during follicular growth, steroidogenesis, and most likely during follicle atresia. BRG1 has been found to interact with H3 at the promoter level in embryos to regulate gene expression controlling cell cycle and apoptosis [13]. Bultman et al. [8] reported that oocyte-specific mutation in BRG1 has no apparent effect on oocyte development, ovulation, or fertilization, but results in a developmental arrest at the two-cell stage. In swine, BRG1 makes its appearance in GCs of secondary follicles [14], highlighting a possible role for BRG1 in the regulation of GC proliferation. Additionally, its expression is stronger in the GCs closest to the theca cells, suggesting a possible role of BRG1 during steroidogenesis, considering the close relationship between granulosa and theca cells for the production of estradiol. Studies have shown that *SMARCA4* is frequently deleted or mutated in a variety of cancer cell lines, which suggests BRG1 can act as a potential tumor suppressor [15].

In this study, we hypothesized that BRG1 has a central role in regulating folliculogenesis and modulating the acquisition of oocyte developmental competence. Using

Cre-LoxP transgenic mouse models, we created conditional knockout (cKO) female mice for *Smarca4*/BRG1 early in oocytes (*Gdf9-Cre*), early in GCs (*Amhr2-Cre*), and late in GCs (*Cyp19-Cre*). Mutation of BRG1 in GCs and oocytes did not cause any tumors, but early depletion in GCs using *Amhr2-Cre* resulted in a full sterile phenotype with possible defects in oocyte quality. Depletion of BRG1 in oocytes using *Gdf9-Cre* resulted in a subfertile phenotype with a reduced number of follicles capable of ovulation. This is the first study to report a possible role for BRG1 during the acquisition of oocyte developmental competence.

Material and methods

Animal models

This study was performed under a protocol approved by the Animal Care Committee of the University of Ottawa and conducted in accordance with the guidelines of the Canadian Council on Animal Care. Mice were housed under controlled environmental conditions with 12-h alternating light/dark cycles, with free access to water and food. To generate *Brg1* cKO in GCs and oocytes, we obtained B6;129S2-*Smarca4*$^{tm1.2Pcn}$/Mmnc (hereafter, *Brg1*$^{fl/fl}$) mice from Dr David Lohnes, with the permission of Dr Pierre Chambon [16]. We also obtained double KO (dKO) with the following genotype *Brg1*$^{f/f}$*/Brm*$^{+/-}$ from Dr Courtney T. Griffin, with the permission of Dr Moshe Yaniv [17]. B6;129S7-Amhr2$^{tm3(cre)Bhr}$/Mmnc (identification number 14245-UNC; hereafter, *Amhr2-Cre*) was obtained from the Mutant Mouse Regional Resource Center, with the permission of Dr Richard Behringer [18]. Tg(*Cyp19a1-cre)1Jri* (hereafter, *Cyp19-Cre*) was obtained from Dr Derek Boerboom (Université de Montreal, Montreal, Canada) [19], and *Tg(Gdf9-icre)5092Coo/J* (hereafter, *Gdf9-Cre*) from Dr Teresa Woodruff (Northwestern University), with the permission of Dr Austin Cooney [20]. Tissue-specific mutant mice with depletion of *Smarca4/Brg1* were generated by crossing *Brg1*$^{fl/fl}$ mice with transgenic mice expressing tissue-specific Cre recombinase. The resulting male mice *Brg1*$^{fl/+}$*;Cre*$^{+/wt}$ were then crossed with female mice to obtain experimental *Brg1*$^{fl/fl}$*;Cre*$^{+/wt}$ female mice (or *Brg1*$^{fl/fl}$*;Gdf9-icre+*, in the *Gdf9-Cre* mutant line*)*, whereas *Brg1*$^{fl/fl}$*;Cre*$^{wt/wt}$ littermate female mice were used as controls. Data originating from control mice are combined between experimental mouse lines as they had the same litter sizes and no difference in phenotypes. Wild-type (WT) male C57BL/6J mice were obtained from The Jackson Laboratory. Genotyping assessments were determined by PCR amplification of mouse ear snip DNA samples. Primers and cycle conditions for each genotyping assessments used in this study are summarized in Supplementary Table 1.

Fertility trials and ovary weights

To assess female fertility, mating experiments were conducted using 8-week-old female mice with the following genotypes: *Brg1*$^{fl/fl}$, *Brg1*$^{fl/fl}$*;Amhr2-Cre,* *Brg1*$^{fl/fl}$*;Cyp19-Cre,* and *Brg1*$^{fl/fl}$*;Gdf9-Cre*, which were mated with 8-week-old WT male mice. Each mating pair was monitored daily and the date and number of pups were recorded at birth for 6 months. Adult males were removed from the cage after 6 months, and the experiment was terminated 22 days after male removal to record the final litter. Ovary weights were obtained from adult cycling mice, aged 6–8 months, and from 21 to 26-day-old mice 44–48 h after intraperitoneal (i.p.) injection with eCG (5 IU, Folligon: Intervert, Whitby, ON, Canada).

Follicle counting, immunohistochemistry, and immunofluorescence

To assess ovarian histopathology, intact ovaries were collected from *Brg1*$^{fl/fl}$, *Brg1*$^{fl/fl}$*;Amhr2-Cre*, and *Brg1*$^{fl/fl}$*;Gdf9-Cre* groups at 2 and 8 months of age. These time points allowed us to determine if fertility is impacted at the start and near the end of their reproductive capacity. Ovaries were fixed in 4% (w/v) paraformaldehyde for 24 h at room temperature and transferred to 70% ethanol to be paraffin embedded. Serial sections were prepared at a thickness of 5 μm, and every fifth section was stained with hematoxylin and eosin (H&E). For follicle assessment on H&E-stained sections, follicles with a visible oocyte nucleus were counted, classified according to Pedersen's system, and scored as healthy or atretic, as previously described in Pedersen and Peters [21]: oocyte surrounded by a layer of flat GCs = primordial, Pedersen Class 3 = primary, Pedersen Classes 4–5 = secondary, and Pedersen Classes 6–8 = antral. Atresia was determined for each follicle based on histological criteria using a weighted scoring system as previously described by Boyer et al. [22]. Briefly, the primary criteria of atresia scoring were: (1) presence and degree of pyknosis (condensed GCs or cells with condensed nuclei), (2) presence and degree of loss of GC attachment to oocytes or loss of cumulus cells, (3) presence of polymorphonuclear neutrophils or lymphocytes, and (4) presence of pyknotic oocytes (primary follicles only). Secondary criteria were GC vacuolation, sparse or missing GCs, and integrity of the basement membrane.

Immunohistochemical analysis of histological sections was performed using an antibody for a marker of cell proliferation, Ki67 (ab16667; Abcam, Cambridge, UK). Sections were incubated with primary antibody at a 1:200 dilution overnight at 4°C. Subsequently, tissue sections were incubated in anti-rabbit horseradish peroxidase-labeled polymer (Dako) for 1 h at room temperature and developed using diaminobenzidine. Sections were lightly counterstained with hematoxylin before mounting with permount (Fisher Scientific). Images were acquired using ScanScope CS2 (Leica Biosystems, Concord, Canada) or using a Zeiss AxioScan Z1 (Zeiss, Oberkochen, Germany). For IHC semi-quantification, images were analyzed using the open-source Orbit Image Analysis software [23]. Briefly, the software uses a machine learning object classification that is built by manually annotating objects to create a classification model. That model was then used for all images to calculate the ratio of positive versus negative KI67-stained cells with the background removed resulting in a ratio relative to WT mice.

Immunofluorescence analysis was performed on fresh frozen ovaries with reproductive tracts from WT female mice at 2 months of age and from control and mutant mice at 8 weeks of age. Ovarian tissues embedded in OCT (Thermofisher, Waltham, MA, USA) were sectioned at a thickness of 10 μm and dried for 30 min on slides at room temperature. Sections were fixed in 4% paraformaldehyde followed by incubations in 0.2% Triton X-100 diluted in PBS for 15 min at room temperature. Slides were rinsed three times PBS and incubated in blocking solution [10% goat serum (G9023, Sigma-Aldrich, St. Louis, MS, USA) diluted in PBS]

for 60 min at room temperature followed by an overnight incubation at 4°C in primary antibodies [rabbit polyclonal anti-Brg1 (NBP2–41270, Novus Biologicals, Littleton, CO, USA) at 5 μg/mL diluted in blocking buffer]. Slides were rinsed three times in PBS and incubated in 4 μg/mL dilution of secondary antibodies in blocking buffer [goat anti-rabbit IgG AlexaFluor 488 (A-11006, Invitrogen, Carlsbad, CA, USA)] for 1 h at room temperature and wash three times with PBS. The slides were mounted with ProLongTM Diamond Antifade Mountant with DAPI (P36962, Thermofisher, Waltham, MA, USA) and coverslipped. We used the Zeiss Axioskop 2 MOT (Oberkochen, Germany) fluorescence imaging microscope at ×40 magnification. Intensity thresholds were set according to the highest intensity image, and tissues from a minimum of three mice were analyzed ($n = 3$).

Oocyte chromatin configuration

Germinal vesicle (GV) oocytes were obtained from 8 to 9 weeks old female *Brg1*$^{fl/fl}$ and *Brg1*$^{fl/fl}$;*Amhr2-Cre* mice, 44–46 h post-eCG (5 IU i.p.) by placing the ovaries in PBS and using a 26-gage needle to puncture the ovaries. Only oocytes fully enclosed by cumulus cells were collected and washed in PBS with gentle agitation until denuded. Oocytes were immediately incubated in 4% paraformaldehyde for 20 min at 37°C, washed three times in PBS, and stained with Hoechst 33342 diluted at 1/300 in PBS for 15 min. Stained oocytes were mounted on slides using mounting media (Immu-mount, Thermofisher) and observed using the Zeiss Axioskop 2 MOT (Oberkochen, Germany) fluorescence imaging microscope at ×40 magnification. Assessment of GV chromatin configuration with non-surrounded nucleus (NSN) or surrounded nucleus (SN) was performed and reported as proportions of SN and NSN oocytes from a minimum of three mice ($n = 3$).

RNA extraction and qRT-PCR

GCs from *Brg1*$^{fl/fl}$ and *Brg1*$^{fl/fl}$;*Amhr2-Cre* genotypes were obtained from immature ovaries 48 h post-eCG. GCs were isolated by placing the ovaries in PBS and using a 26-gage needle to puncture the ovaries to extract GCs. GCs were filtered by a 40 μm cell strainer to separate GCs and oocytes. GCs were collected and centrifuged at 2000 RPM and frozen at −80°C until RNA extraction. Oocytes from the *Brg1*$^{fl/fl}$ and *Brg1*$^{fl/fl}$;*Gdf9-Cre* genotypes were obtained by collecting the cumulus oocyte complexes (COCs) after ovarian puncture. Hyaluronidase was used to remove the cumulus cells immediately after collection, and denuded oocytes were collected and frozen at −80°C until RNA extraction. Total RNA from the GCs and oocytes was extracted using the RNeasy Mini kit (#74106, Qiagen) according to the manufacturer's protocol. Reverse transcription was performed with 200 ng GC RNA and 30 ng oocyte RNA using an iScript cDNA Synthesis Kit (Bio-Rad, Mississauga, ON, Canada). Real-time PCR was performed with Fast SYBR Green Master Mix (Invitrogen, Carlsbad, CA, USA). Each PCR reaction consisted of 5.5 μl of Fast SYBR Green Master Mix, 2.5 μl of RNAse free water, 1 μl of cDNA sample, and 0.5 μl (10 pmol) of *Smarca4*-specific primers (Supplementary Table 1). The qPCR was run using the 7500 Fast system assays (Applied Biosystems). To quantify relative gene expression, the cycle threshold (Ct) of target gene amplification was normalized to the expression level of a housekeeping gene (*Actin*) using the delta–delta Ct method.

Assessment of ovulation

To determine the natural ovulation rates, 8–10-week-old females of experimental and control genotypes were housed with WT males of proven fertility and monitored daily for the presence of a vaginal plug. For assessment of the number of COCs after superovulation, immature mice were injected with eCG for 48 h prior to hCG injection (5 IU i.p., Chorulon; Intervet) and COCs were collected after 14 h. For both natural matings and superovulation, the animals were euthanized and the oviducts were removed and placed in sterile saline under a dissection microscope. COCs were released by tearing open the ampullae of the oviducts with forceps and were counted.

Steroid hormone measurement

Blood samples were collected by cardiac puncture before euthanasia. Estradiol (E2) and progesterone (P4) levels in the serum were measured by Calbiotech and IBL ELISA, respectively. All assays were performed by the Ligand Assay and Analysis Core Laboratory of the University of Virginia (Charlottesville, VA, USA).

Embryo culture and imaging

Embryos were obtained from female *Brg1*$^{fl/fl}$ and *Brg1*$^{fl/fl}$; *Amhr2-Cre* mice (age: 8–10 weeks) that had been naturally mated with a fertile WT male. Two-cell embryos were flushed from excised oviducts ~1.5 days after mating (after observation of vaginal plug) with fresh washing media (KFHM). Two-cell embryos were cultured in embryo culture media (KSOM) overlaid with mineral oil at 37°C in 5% CO_2 in air (designated as Day 1), and the number of four-cells or greater on Day 2, morula on Day 3, and blastocyst formation on Day 4 was recorded. For imaging, embryos were fixed with 4% (w/v) paraformaldehyde for 30 min at 37°C and permeabilized (0.25% triton-X 100). They were then stained with phalloidin 488 and Hoechst followed by imaging with a Zeiss 880 confocal microscope (Cell Biology and Image Acquisition core, University of Ottawa). Embryos were imaged with a ×40 oil immersion objective. Z-slices of 2 μm were captured across the whole embryo and scored using ImageJ (Fiji) software.

RNA sequencing data retrieval

RNA sequencing data from a previous study of human folliculogenesis assessing gene expression in GCs and oocytes (GSE107746) were retrieved from the Gene Expression Omnibus website (https://www.ncbi.nlm.nih.gov/geo). Expression levels of *SMARCA4* were directly extracted from a transcriptomic study of the human ovary and are provided in fragments per kilo-million mapped reads (FPKM) plus one then log2 transformed from GCs and oocytes originating from the same follicular stage [24]. RNA sequencing data from cow early embryonic development were retrieved from EmbryoGENE profiler website (https://emb-bioinfo.fsaa.ulaval.ca/IMAGE/). Briefly, transcript abundances in FPKM were normalized against the spiked synthetic transcriptome ERCC abundances in each library to obtain an absolute estimate of gene expression, which can be compared between developmental stages [25]. RNA-seq data sets were not reanalyzed but were statistically evaluated for differences in expression between follicle stages using an ANOVA with Tukey's multiple comparison test.

Statistical analyses

All statistical analyses were performed using Prism 9 software (GraphPad Software Inc., La Jolla, CA, USA). Data sets were compared using *t*-test, two-tailed *t*-test with Mann–Whitney post hoc, or ANOVA (with Tukey's or Dunnett's multiple comparisons posttest) when specified. All data are presented as means ± SEM.

Results

Smarca4 is expressed in GCs and oocytes throughout folliculogenesis and early embryogenesis

To investigate the expression pattern of *SMARCA4*, we used data from a previous RNA sequencing analysis of human GCs and oocytes and verified the expression during folliculogenesis and oogenesis [24]. *SMARCA4* is expressed at all stages of human folliculogenesis in both GCs and oocytes with significantly increased expression in GCs with stage of follicle progression and a sharp decrease in oocytes in secondary follicles relative to the other stages (Figure 1A and B). Using data from a previous RNA sequencing study on bovine early embryonic development [26], we noted that *SMARCA4* tends to decrease before the ZGA, which occurs at the eight-cell stage in cows [27]. Interestingly, *SMARCA4* expression is significantly increased in the expanded blastocyst compared with eight-cells and morula (Figure 1C). These analyses show that *SMARCA4* is expressed early during folliculogenesis and oogenesis and is also strongly expressed in the embryo following the ZGA, supporting its role in the embryonic development in cows and women. We then stained WT mouse ovaries for BRG1 by immunofluorescence to assess the spatial expression within the ovary. BRG1 was detectable in GCs at all stages of follicular development, similar to other species, but was also expressed in the stroma, theca cells, and in the luteinized GCs. Interestingly, BRG1 expression was also detected specifically in the epithelium of the oviduct and uterus (Figure 1D).

Smarca4 expression is successfully reduced in cKO mutant mice

To delete the *Smarca4*/BRG1 from GCs and oocytes, we used conditional recombination of *Brg1* floxed/floxed mice crossed with mice heterozygous for a "knock-in" allele containing a Cre-Neo cassette inserted into *Amhr2* [18], denoted as *Amhr2-Cre* or crossed with transgenic mice with *Cyp19* or *Gdf9* promotor ligated to iCre cDNA [19, 20], denoted *Cyp19-Cre* and *Gdf9-Cre*, respectively. Cre-mediated recombination occurs at different time points during folliculogenesis, depending on the timing of activation of the allelic promoters. Briefly, Cre activity in *Amhr2-cre* mice was reported as early as embryonic day e11.5 in female urogenital ridges and at embryonic day e12.5 in gonads and Müllerian ducts [28]. In postnatal ovaries, *Amhr2-Cre* activity was reported in GCs of all secondary and antral follicles, with lower to no detection in primordial and primary follicles. However, low Cre activity was also found in theca cells, oocytes [28], and in the ovarian surface epithelium (OSE) [29]. In the postnatal ovaries, *Cyp19-Cre* activity was reported in GCs of all antral follicles and most luteal cells with undetectable expression in primordial/primary follicles, theca cells, oocytes [19], or OSE [29]. Cre activity in *GDF9-cre* mice was reported as early as the primordial follicle stage in 3-day-old mice and older with no expression in somatic cells [20]. The conditional recombination of *Brg1* by Cre is performed using a Cre-LoxP system for which LoxP sites had been inserted in the introns located upstream of exon 17 and downstream of exon 18 [16]. Using RT-qPCR, we designed primers specific to Exons 17 and 18 of the *Smarca4* gene (Supplementary Table 1) and confirmed the reduced expression of *Smarca4* transcripts in GCs from the *Amhr2-Cre* and *Cyp19-Cre* mutant mice at 48 h after eCG and in oocytes from the *Gdf9-Cre* mutant compared with the appropriate control mice (Figure 2A–C). We performed immunofluorescence and confirmed the depletion of BRG1 in GCs from antral follicles from the *Amhr2-Cre* and *Cyp19-Cre* mutant mice and found no expression in oocytes from the *Gdf9-Cre* mutant (Supplementary Figure 1).

Conditional KO of BRG1 using Amhr2-Cre and Gdf9-Cre in female mice results in sterility and subfertility, respectively

To investigate the effect of maternal BRG1 on female fertility, we conducted a breeding study over a period of 6 months. Eight-week-old WT (C57BL/6) males were mated with 8-week-old control mice ($Brg1^{fl/fl}$), somatic cell mutants ($Brg1^{fl/fl}$;*Amhr2-Cre* and $Brg1^{fl/fl}$;*Cyp19-Cre*), and germ cell mutants ($Brg1^{fl/fl}$;*Gdf9-Cre*). Number of litters and size were documented (Figure 3A). None of the six female Amhr2-Cre mutant mice had any pups and were classified as sterile. The six Gdf9-Cre mutant females had a total of 26 litters with only 102 pups for an average of 4.02 pups per litter, which was significantly fewer than control mice. Linear regression on the number of pups per litter over time shows no significant change in the slope, but did show a significant difference in the intercept compared with control mice (Figure 3B), reflecting an earlier onset of the decline in fertility. Interestingly, the fertility of Gdf9-Cre female mice did not have the increase in litter size normally seen during the first 2–3 months following pairing with a fertile WT male. Instead, their fertility decreased from the start.

Fertility of female mice with Cyp19-Cre recombination was not significantly different from control mice. Since it has been previously reported that BRM might compensate for BRG1 loss [8], we tested this possibility by crossing the $Brg1^{fl/fl}$;*Cyp19-Cre* mouse model to *Brm null* mice. Female mice with dKO for both BRM and BRG1, noted as $Brm^{-/-}$;$Brg1^{fl/fl}$;*Cyp19-Cre*, showed no differences in fertility compared with control mice (Figure 3C). Henceforth, data from Cyp19-Cre will not be shown because of lack of any apparent phenotype. Our results suggest that depleting BRG1 in GCs early during folliculogenesis negatively impacts fertility, whereas later depletion, during the preovulatory stage, has no impact on fertility. Since deleting BRG1 early in oocyte growth decreased by half the number of pups, rendering these mice sub-fertile, we further explored the stages of development where defects became apparent.

BRG1-deficient oocytes are associated with fewer ovulations

To investigate whether the reduced reproductive performance of *Brg1* cKO female might be explained by an ovulation deficiency, we counted the number of ovulated COCs in mutant mice ($Brg1^{fl/fl}$;*Amhr2-Cre* and $Brg1^{fl/fl}$;*Gdf9-Cre*) following either natural mating or superovulation. Naturally mated

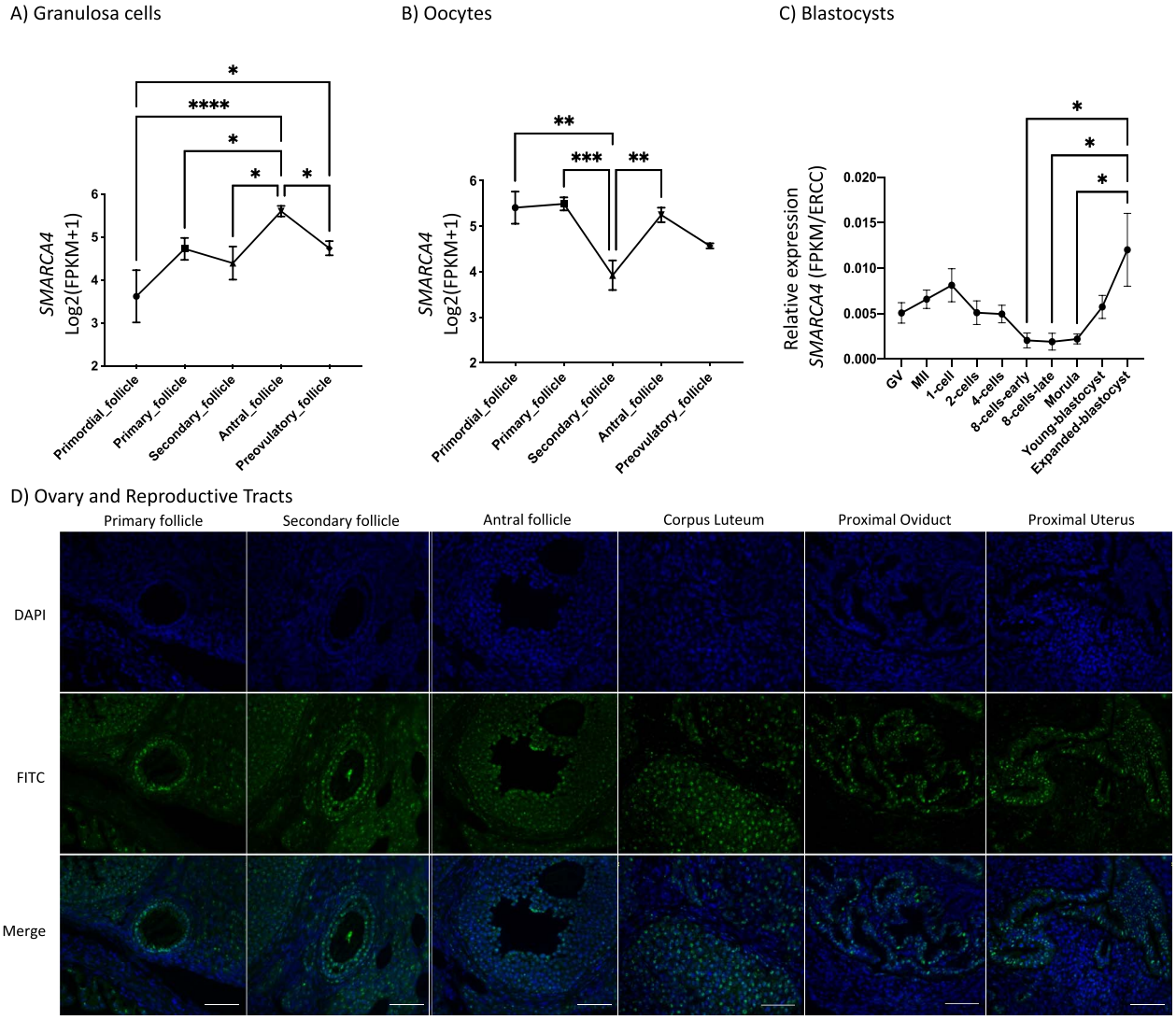

Figure 1. *SMARCA4*/BRG1 is expressed during female reproduction. *SMARCA4* expression level in FPKM mapped reads plus 1 then log2 transformed from normalized RNA-seq data of human GCs (A) and oocytes (B) originating from primordial, primary, secondary, antral, and preovulatory follicles from women. (C) Time course expression of *SMARCA4* in cow early embryo development in relative expression, total FPKM abundances normalized against the ERCC synthetic transcriptome abundances (Life Technologies). (D) Immunofluorescence of BRG1 (FITC) and DAPI in ovaries and reproductive tracts from WT mice at 2 months of age. Separate channels and a merge are shown at ×40Xmagnification, scale bar is 55 μm and a minimum of three samples of each genotype have been analyzed (*$P < 0.05$, **$P < 0.01$, ***$P < 0.001$).

female mice (2 months old) were euthanized after observation of the vaginal plug and COCs in the ampulla were counted. In naturally mated mice, there was no difference in total number of COCs per mouse in Amhr2-Cre mutants (mean 7.60 ± 0.67) compared with control mice (mean 7.16 ± 0.87) but a significant reduction to about half the number of COCs from *Gdf9-Cre* mutant mice (mean 3.70 ± 0.62) (Figure 3D). Similar results were found in the superovulated immature mice, where the Amhr2-Cre mutant mice showed no difference (mean 38.50 ± 6.94) in the total number of COCs compared with controls (mean 36.50 ± 2.59), but the number of COCs was significantly reduced in the *Gdf9-Cre* mutant mice (mean 14.00 ± 2.30) (Figure 3E). The results of these experiments suggested that the defect in *Amhr2-Cre* mutant mice occurs after ovulation, whereas *Gdf9-Cre* mutant mice have deficiencies in follicular growth and/or ovulation.

BRG1 cKO female mice have ovarian histologic anomalies

To identify whether the ovulation anomalies in *Gdf9-Cre* mutant mice are associated with poor follicular development or failed ovulation, we compared the ovaries of control mice with those of *Amhr2-Cre* and *Gdf9-Cre* mutant mice. Mutant mouse ovaries were significantly heavier compared with control mice in both immature (21–26 days) and adult cycling mice (6–8 months) (Supplementary Figure 2A). We also noted the occasional presence of luteinized follicles in immature ovaries of *Gdf9-Cre* mutant mice only (Supplementary Figure 2B).

The number of primordial follicles showed no obvious differences between the groups at the two different ages assessed, 2 and 8 months (Figure 4A and B). However, the number of primary follicles was significantly higher in younger mutant mice and significantly lower in older mutant mice compared

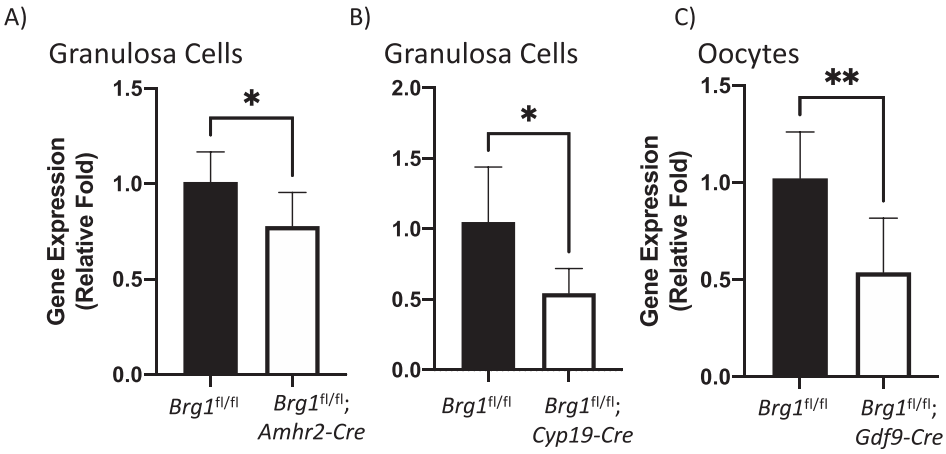

Figure 2. *Brg1* is effectively knocked down in mutant mice. (A–C) Expression of *Brg1* was determined by RT-qPCR in GCs and oocytes isolated from immature eCG-treated mice of the indicated genotypes, *Brg1*$^{fl/fl}$;*Amhr-Cre, Brg1*$^{fl/fl}$;*Cyp19-Cre* and *Brg1*fl/fl;*Gdf9-Cre* models ($n = 5$ animals/time point). Data are means ± SEM. $^{*}P < 0.05$, $^{**}P < 0.01$.

A)

	Brg1(fl/fl)	*Brg1(fl/fl);Amhr2-Cre*	*Brg1(fl/fl);Cyp19-Cre*	*Brg1(fl/fl);Gdf9-Cre*
Total litters	33	0	32	26
Total pups	219	0	231	102
Litter size	6.70 ± 0.32	0****	7.16 ± 0.39ns	4.02 ± 0.44**

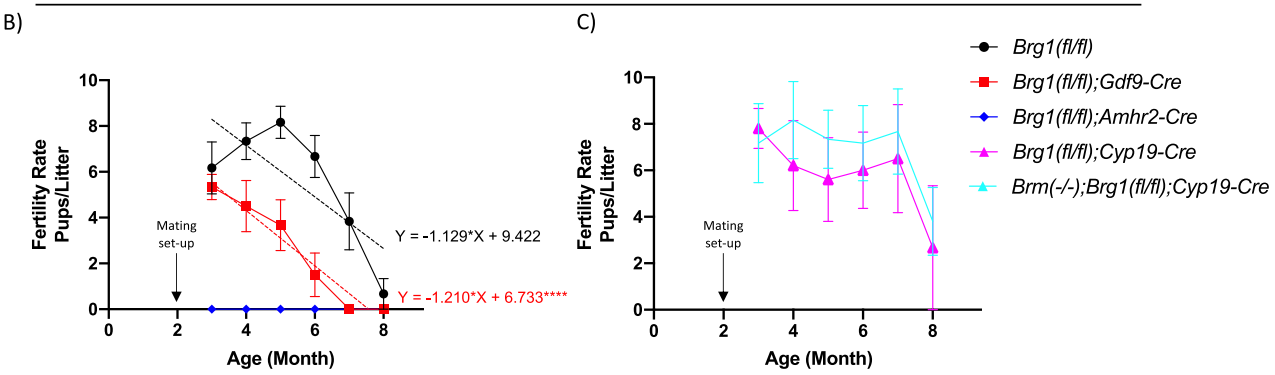

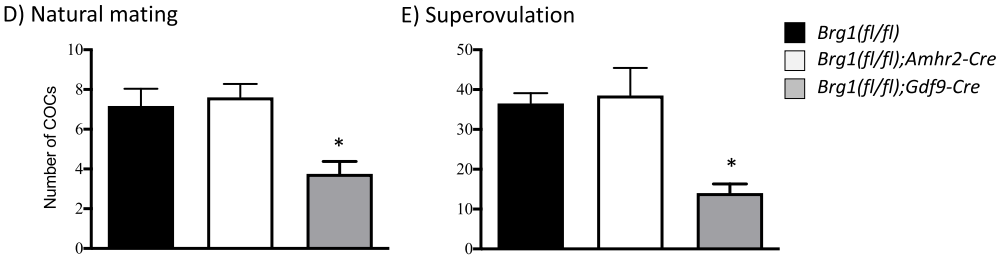

Figure 3. *Brg1* mutant mice have altered reproductive performances and ovulation capability. (A) Fertility data of the control group *Brg1*$^{fl/fl}$, and *Brg1*$^{fl/fl}$;*Amhr2*-Cre, *Brg1*$^{fl/fl}$;*Cyp19*-Cre and *Brg1*$^{fl/fl}$;*Gdf9*-Cre mice are presented. Total litters and total pups are the total of $n = 6$ pairs per group. Each female mouse was bred with a fertile WT male for a period of 6 months and the number of pups was counted after each birth. Litter size refers to the average number of pups per litter. Differences in litter size compared with control group were analyzed using one-way ANOVA with Dunnett multiple comparison test. Data are means ± SEM. (B) Fertility rate gradually decreased over fertility trial period in *Brg1*$^{fl/fl}$;*Gdf9*-Cre mice compared with control group. Simple linear regressions are shown in dashed black and red lines with their respective equation. Intercepts are significantly different between groups. (C) Fertility rate in *Brm*$^{-/-}$;*Brg1*$^{fl/fl}$;*Cyp19-Cre* is not different from single-*Brg1*$^{fl/fl}$;*Cyp19*-Cre knockout and *Brg1*$^{fl/fl}$ control mice. (D, E) Number of COCs counted after ovulation in naturally cycling females and after superovulation from three female mice per genotype. Data are presented as means ± SEM and analyzed using ANOVA with Dunnett's multiple comparison test ($^{*}P < 0.05$, $^{**}P < 0.01$, and $^{****}P < 0.0001$, ns = not statistically different).

with controls. The same tendency occurred for the number of secondary follicles but not for the tertiary follicles. Female mice from the *Gdf9-Cre* genotype had decreased numbers of tertiary (antral) follicles at both ages and increased numbers of atretic follicles. Although similar in trend, that difference was not significant for female mice of the *Amhr2-Cre* genotype.

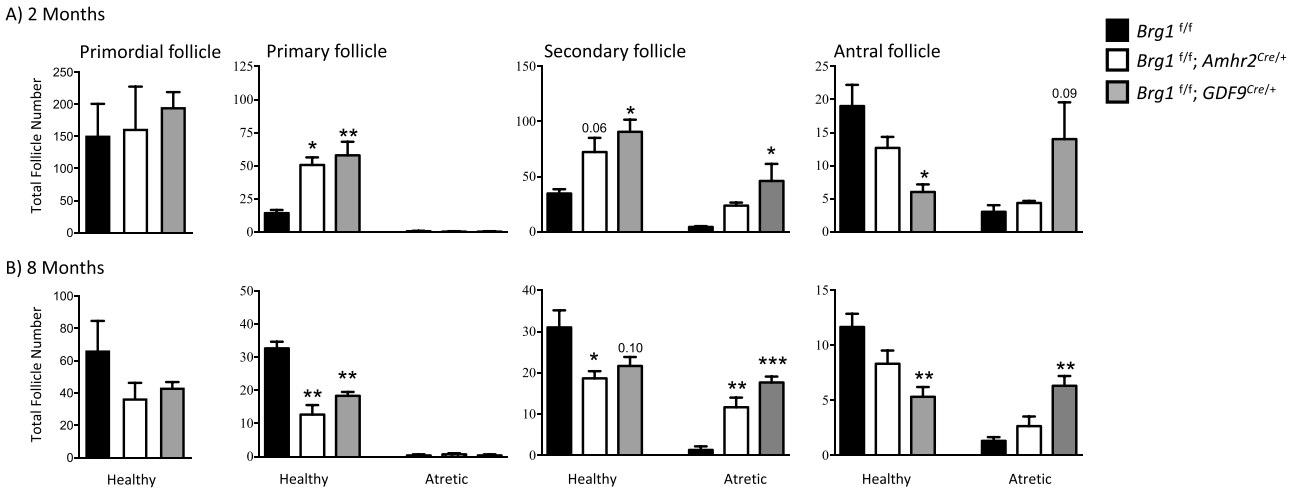

Figure 4. *Brg1* mutant mice show variations in the proportions at each follicle stage. Follicle numbers at different stages in the ovaries of *Brg1*$^{fl/fl}$ (black bars), *Brg1*$^{fl/fl}$;*Amhr2-Cre* (white bars) and *Brg1*$^{fl/fl}$;*Gdf9-Cre* (gray bars) at (A) 2 months and (B) 8 months were counted. Left ovaries from each indicated genotype ($n = 3$) were serially sectioned, and all follicles with visible nucleus from every fifth section were counted, categorized (primordial, primary, secondary, and tertiary), and scored (healthy or atretic). Data were analyzed using one-way ANOVA with Dunnett's multiple comparison test to compare significance against the control group. Data are means ± SEM (* $P < 0.05$, ** $P < 0.01$, *** $P < 0.001$).

Overall, the histologic analysis showed that *Gdf9-Cre* mutant mice, despite having more follicles activated to grow, are disrupted late in follicle development, resulting in fewer healthy antral follicles and therefore fewer ovulations. Interestingly, *Amhr2-Cre* mutant mice also activated more follicles but retained enough to become healthy antral follicles with no apparent impairment in ovulation.

BRG1 plays a role in female steroidogenesis

Since follicular growth is abnormal in mutant mice, we investigated if steroid hormone production was affected by BRG1 cKO. Serum hormone assays revealed a significant decrease in E2 production in *Gdf9-Cre* mutant mice compared with control mice, but no difference in *Amhr2-Cre* mutant mice neither after eCG nor after injection of both eCG and hCG. In contrast, both mutants showed a significant increase in progesterone levels following eCG and hCG compared with control mice (Figure 5A). To determine if there might be an association between steroid hormone levels in response to gonadotropin stimulation and changes in *Smarca4* expression in normal ovaries, we performed RT-qPCR on GCs from WT mice and found that the post-hCG decrease in E2 levels was associated with increased expression of *Smarca4* (Figure 5B).

BRG1 null GCs lead to poor oocyte quality

The follicle assessment shows that there are no differences between control and *Amhr2-Cre* mice in terms of healthy and atretic antral follicles and ovulations. We also found no significant difference in GV chromatin configuration between the control and *Amhr2-Cre* mutant mice (Supplementary Figure 3). To further investigate whether the infertility phenotype of the *Amhr2-Cre* mice might be explained by an embryonic phenotype, we collected and cultured two-cell embryos from 2-month-old *Brg1*$^{fl/fl}$ control mice and *Brg1*$^{fl/fl}$;*Amhr2-Cre* mutant mice after natural mating with a WT male mouse. Figure 6A shows images of each developmental stage between two-cell embryos to the formation of blastocysts. There was no difference in the number of collected two-cell embryos between both groups, but the number of healthy blastocysts in the *Amhr2-Cre* group (mean 0.6 ± 0.40) was significantly reduced compared with the control group (mean 5.16 ± 0.47) (Figure 6B). We also noted that 83.7% of two-cell embryos collected from control mice reached blastocysts but only 7.89% of two-cell embryos from mutant mice developed into blastocysts (mean 7.60 ± 0.67 versus mean 0.60 ± 0.40). We then collected and cultured embryos from both control and *Amhr2-Cre* mutant mice to assess any anomalies under confocal microscopy. Figure 6C shows images of morulas stained for DNA and actin to better identify mitotic rates by counting cells in metaphase division and to assess micronuclei (mn), which are extra-nuclear bodies that contain damaged chromosome fragments because of mitotic defects. We discovered that embryos originating from mutant female mice had higher numbers of micronuclei per embryo (mean 4.82 ± 0.5 versus mean 2.68 ± 0.51) and also had higher cell counts compared with controls (mean of 50 ± 2.53 versus mean 41 ± 3.39). Although the mitotic index was slightly lower and the number of micronuclei per cell was slightly higher, neither difference was significant (Figure 6D–G). The greater abundance of extra-nuclear DNA suggests mitotic division errors, which may contribute to the failure to form viable blastocysts. Since it is known that accelerated follicle growth contributes to reduced oocyte quality [30], we sought to compare the rates of GC proliferation in association with follicle state in the GC mutant mice. As expected, the rate of proliferation of GCs in *Amhr2-Cre* mutant mice was higher in both primary and antral follicles, as shown by immunostaining (IHC) for Ki67 (Figure 7).

Discussion

In a reproductive context, BRG1 has been described to function as a maternal-effect gene essential for the ZGA that occurs during embryogenesis [8]. It also plays a crucial role in tissue-specific gene regulation during embryonic development [31]. Currently, little is known about the role of BRG1 during folliculogenesis and oogenesis, but identifying the resultant

A)

Hormone	*Brg1*(f/f)	*Brg1*(f/f);*Amhr2*-Cre	*Brg1*(f/f);*Gdf9*-Cre
48h post eCG			
E2(pg/ml)	74.10±0.68[a]	83.37±0.62[a]	17.35±0.65[b]
P4(ng/ml)	10.75±1.90	10.06±1.06	11.13±1.48
48h eCG followed by 14h post hCG			
E2(pg/ml)	7.8±2.6	4.97±1.5	5.16±1.32
P4(ng/ml)	11.55±0.73[a]	18.74±2.68[b]	18.30±2.72[b]

B) Granulosa Cells

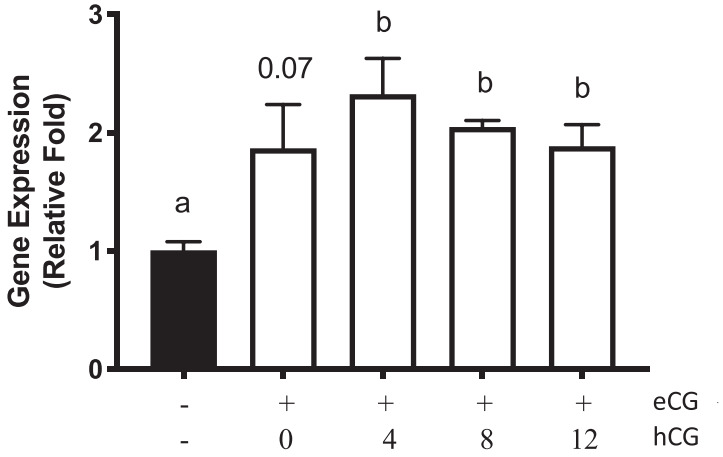

Figure 5. Estradiol and progesterone production are impaired in *Brg1* mutant mice. (A) Serum levels of estradiol (E2) and progesterone (P4) were measured in blood samples of immature mice (21–26 days) 48 h after eCG injection (5 IU, i.p.) or 48 h eCG followed by 14 h post-hCG. Data are means ± SEM. *n*, minimum of 4 mice per group. (B) In vivo regulation of *Brg1* mRNA levels in GCs by gonadotropins in immature (21–26-day-olds) WT female mice injected with eCG (5 IU, i.p.) 44–48 h before the administration of hCG. [a,b] Different superscript letters indicate significant differences between control group and indicated genotypes, $P < 0.05$.

phenotype in which BRG1 plays an essential role may lead to a better understanding of follicle development and its impact on the acquisition of oocyte developmental competence. In this study, we reported the phenotypic effect of three cKO of BRG1 in somatic cells and germ cells, and provide the first evidence that loss of BRG1 can impact proper folliculogenesis, steroidogenesis, ovulation, and the ability of the fertilized oocyte to develop into a healthy blastocyst.

In a previous study, BRG1-depleted oocytes using *Zp3-Cre* were meiotically competent and capable of being fertilized but embryos conceived from such eggs exhibited higher ZGA defects [8] and did not develop past the blastocyst stage [32]. Depleting BRG1 earlier in oogenesis using *Gdf9-Cre* limited the growth of follicles with impaired oocytes, possibly by activating follicular atresia. We also noted that immature Gdf9-Cre ovaries occasionally harbored follicles with luteinized cells, which is suggestive of premature GC luteinization. We have previously observed this phenotype in *Smarca1/Snf2L*-deficient mice [7], and Pangas et al. [33] reported that granulosa deficiency in Smad4 also resulted in premature luteinization, which they attributed to interruption in the communication between oocytes and GCs. Both these studies also documented increases in progesterone levels, similar to what we observed in this study. It is also possible that not all oocytes expressed sufficient Cre to cause *Brg1* deletion and those that did not are the ones that were able to ovulate. Taken together, we suggest that BRG1 is required for proper oocyte development and its depletion causes defects in folliculogenesis that appeared to be the cause of the subfertility in female *Gdf9*-mutant mice.

The functional role of BRG1 in GCs is yet to be discovered but, using RNA sequencing data from human ovaries [24], we found that *SMARCA4* gene expression shows a continuous increase during follicle growth, reaching its highest levels at the antral follicle stage. Interestingly, the follicular transition from primordial to primary is characterized by the acquisition of proliferative capacity in GCs [34], and this coincides with the timing of the appearance of BRG1 protein in mouse and porcine GCs determined by immunofluorescence [14]. We demonstrated higher expression of a proliferation

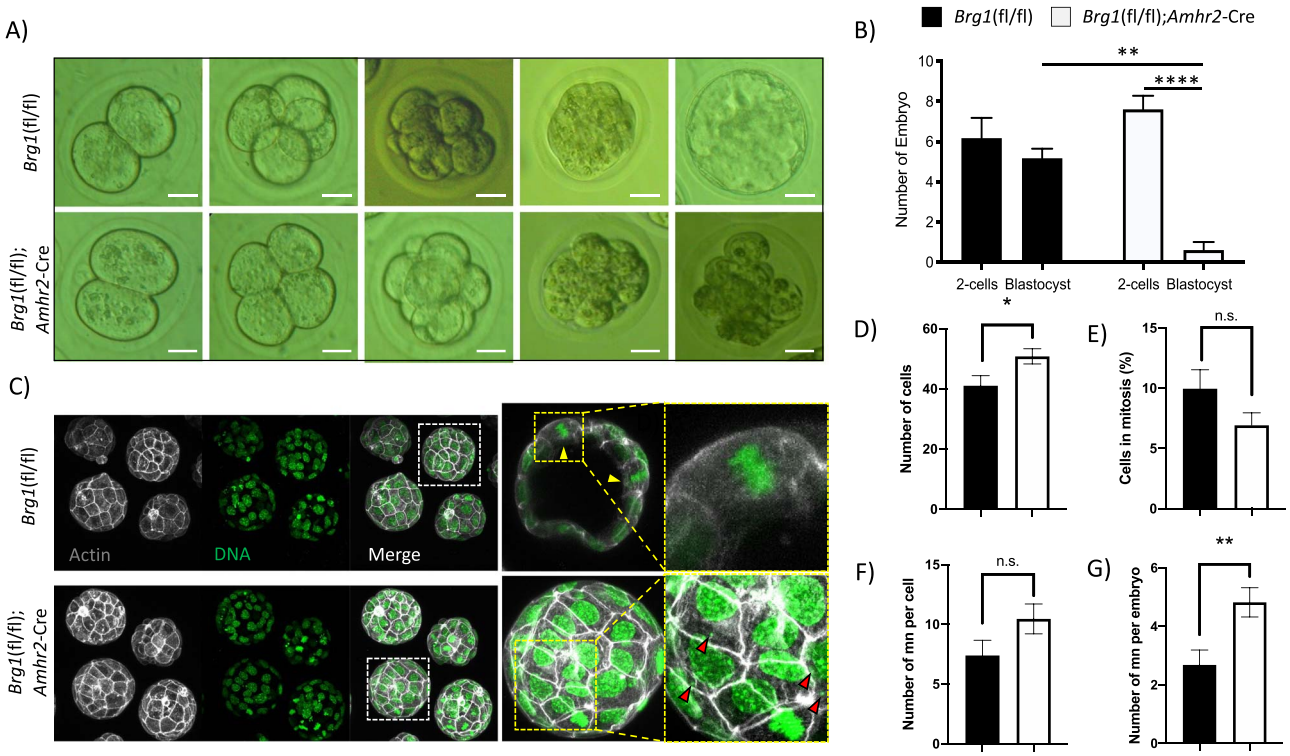

Figure 6. BRG1 depletion in GCs prevents the formation of healthy blastocysts. (A) Morphological comparison of embryonic developmental stages from two-cell embryos to blastocysts in *Brg1*$^{fl/fl}$ and *Brg1*$^{fl/fl}$*;Amhr2-Cre* mice after natural mating ($n = 3$). Scale bar, 50 μm. (B) Number of two-cell embryos retrieved and cultured in vitro in association with the number of blastocysts recorded at Day 3. Data are presented as means ± SEM and analyzed using ANOVA with Tukey's multiple comparison test. (C) Embryos of transgenic mice Brg1$^{fl/fl}$ and *Brg1*$^{fl/fl}$*;Amhr2-Cre* from in vitro culture after superovulation and mating. Maximum intensity projections of embryos stained for actin (gray) and DNA (green). Image enlargements from dotted squares show metaphase (top right) and micronuclei (bottom right using red arrows) detection. (D–G) Embryos were scored for their number of cells, percentage of cells in mitosis, number of micronuclei per cell, and number of micronuclei per embryo. Data are presented as means ± SEM and analyzed using *t*-test (*$P < 0.05$, **$P < 0.01$, ***$P < 0.001$).

marker in the BRG1-depleted primary and antral follicles, suggesting that BRG1 may regulate GC proliferation. *Brg1* gene expression is increased under eCG and hCG stimulation in immature mice, supporting possible roles for BRG1 in modulating GC proliferation and differentiation. It is well accepted that *Brg1* is predominantly expressed in cell types that constantly undergo proliferation or self-renewal [35, 36] and binds to promoters of cell cycle-dependent genes to modulate the cell cycle in various tissues [37, 38]. Specifically, pRB recruits BRG1 to suppress transcription by remodeling chromatin structure and to efficiently block cells in the G1 phase thereby inducing cell cycle arrest [39–41]. Moreover, BRG1-deficient cells show aberrant cell cycle checkpoint activation and that cell cycle arrest is not observed [42]. Our results suggest that BRG1 depletion is associated with accelerated GC proliferation, which appears to impair the acquisition of developmental competence in the resultant oocyte. This agrees well with previous studies showing that ovarian stimulation is associated with detrimental reproductive effects, including decreased rates of embryonic development and increased rates of chromosomal abnormalities [43–45]. Blondin et al. [30] proposed that accelerated follicular growth induced by ovarian stimulation in cows yields oocytes with decreased developmental competence, possibly because of incomplete oogenesis. In mice, accelerating growth of isolated oocyte–GC complexes in vitro using FSH and/or insulin had deleterious effects on the percentage of oocytes that developed to the blastocyst stage [46]. These studies reinforce the importance of timing and adequate follicle growth in relation to oocyte quality.

Our data show that deficiency of *Brg1* in GCs is not associated with any changes in GV chromatin configuration, which is similar to the expected ratio in WT female mice [47, 48] but it does lead to increased numbers of micronuclei and an abnormal mitosis rate in resultant embryos. Similar observations have been reported in fibroblast cell lines in which *Brg1* deletion increased the appearance of micronuclei and aberrant mitosis [49] and using siRNA targeting *Brg1* in HeLa cells, which resulted in mitotic abnormalities [50]. Interestingly, knockdown of ATRX in oocytes, another member of the SWI/SNF2 family, was associated with higher incidence of micronuclei and chromosome segregation defects during embryo development [51]. These data suggest that SWI/SNF complexes in GCs are essential for controlled cell cycle and appear to support the proper acquisition of oocyte quality and capacity for embryonic development, although how GCs convey that impairment to oocytes remains to be elucidated. While this is the more likely interpretation of the results, it should be noted that the embryos resulting from an Amhr2-Cre female and a WT male would have only one WT /functional allele of *Brg1*, such that the phenotype could also be because of haploinsufficiency in the embryo.

There is one comment that should be made on the consequences of *Smarca4*/*Brg1* depletion in the ovary. There is a rare and aggressive form of ovarian cancer called small cell carcinoma of the ovary, hypercalcemic type (SCCOHT)

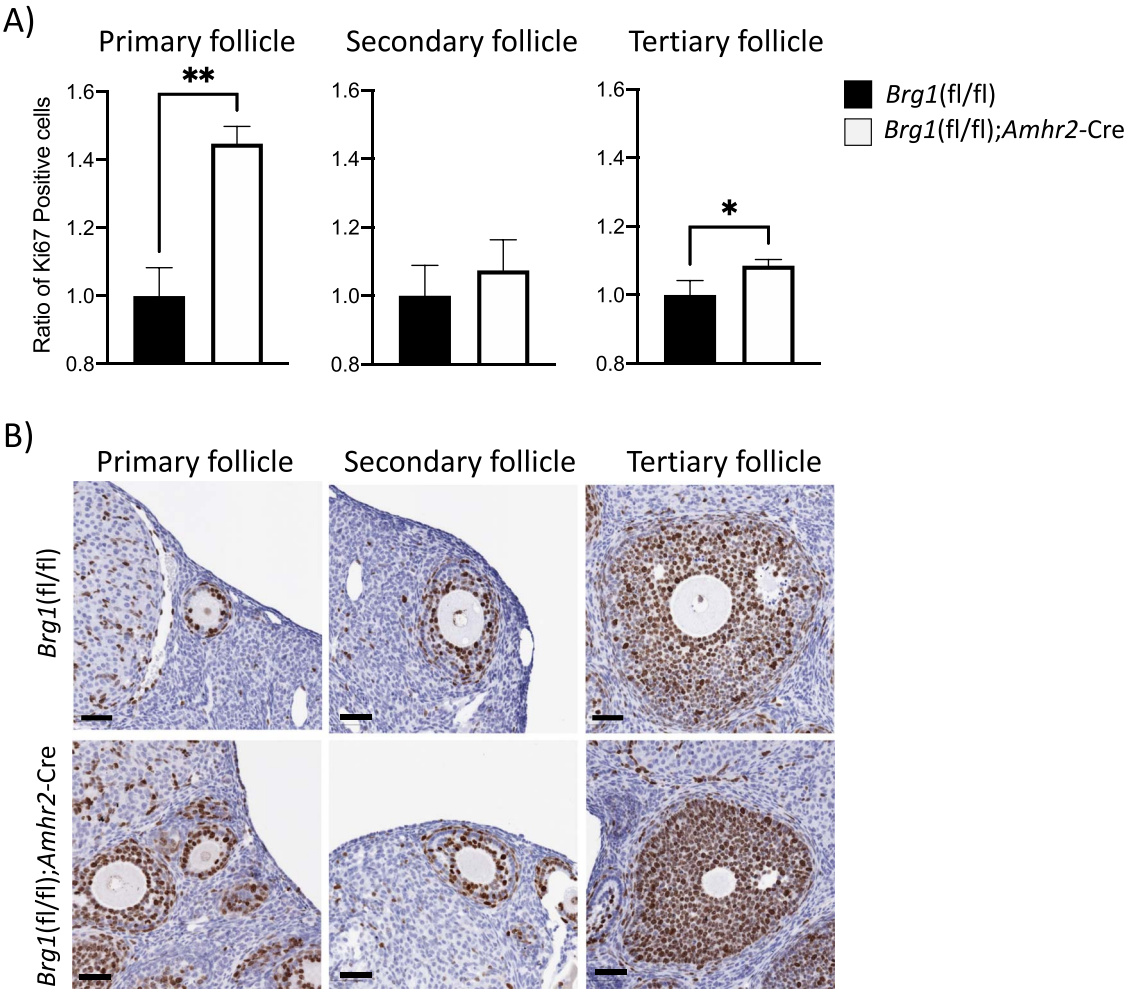

Figure 7. BRG1 depletion increased proliferation of GC semi-quantitative analysis of immunohistochemistry for Ki67. Staining images were analyzed using Orbit Image Analysis software to calculate the ratio of Ki67 positive and negative cells in *Brg1*$^{fl/fl}$ ($n = 3$) and *Brg1*$^{fl/fl}$;*Amhr2-Cre* ($n = 3$) mice in association to follicle developmental stage. Data are means ± SEM (* $P < 0.05$, ** $P < 0.01$, *** $P < 0.001$).

that affects primarily young women (median 23.9 years) and has a poor prognosis [52]. The etiology is unknown and it remains unclear which ovarian cell type is the origin of these tumors. Unlike most ovarian cancers, SCCOHT tumors are genomically stable [53], and it has been previously shown that almost all SCCOHT share a single anomaly—a mutated *SMARCA4* gene [54–57]. It was therefore part of the rationale of this study to determine if *Brg1* depletion in the oocytes, GCs, or OSE might result in tumor formation, and none of them did. While this does suggest that none of these cell types is the SCCOHT cell of origin, it is also possible that the single depletion was not sufficient to promote tumor formation or that depletion in mouse ovaries is not as harmful as in human tissues.

Conclusion

SWI/SNF chromatin remodeling complexes are one of the most dynamic mechanisms of gene expression regulation. As one of the two core subunits, BRG1 plays an important role in normal cell function, proliferation and division. Our results suggest that BRG1 is essential to regulate folliculogenesis and its depletion negatively impacts female fertility. We provide evidence to show that BRG1 is involved during GC proliferation and is associated with oocyte quality, as assessed by its capacity for embryonic development. While depletion of BRG1 in the Amhr2-Cre model could also occur in the uterus, the failure of preimplantation embryo development precluded any assessment of the uterine contribution to the infertility phenotype. Future analyses will need to examine potential the specific molecular defects associated with *Brg1* mutation, e.g. by RNA-seq of GCs and isolated oocytes.

Supplementary material

Supplementary material is available at *BIOLRE* online.

Data availability

The data underlying this article are available in the article and its online supplementary material. The data sets are available in Gene Expression Omnibus and can be assessed with the unique identifier GSE107746 and from EmbryoGENE profiler website (https://emb-bioinfo.fsaa.ulaval.ca/IMAGE/).

Acknowledgements

We thank Dr. David Lohnes, Dr. Derek Boerboom, Dr. Teresa Woodruff, and Dr. Courtney Griffin for providing the experimental mice for this study.

Conflict of interest

The authors have declared that no conflict of interest exists.

Author contribution

A.A., D.A.L., and B.C.V. conceived the study and interpreted the results. D.A.L. and B.C.V. wrote the manuscript. D.A.L., A.A. H.V., A.P., D.I., R.S., V.M., E.M., and B.C.V. reviewed the manuscript. A.A., D.A.L, A.M., V.M., and E.M. performed mouse experiments, embryo culture, and embryo imaging. D.A.L., A.A., H.V., A.P., D.I., and R.S. performed tissue collection, histologic analysis, primer confirmation, qPCR, IHC, IF, and imaging. D.A.L. performed all statistical and computational analyses.

References

1. Sirard M-A, Richard F, Blondin P, Robert C. Contribution of the oocyte to embryo quality. *Theriogenology* 2006; **65**: 126–136.
2. Landry DA, Sirard M-A. Follicle capacitation: a meta-analysis to investigate the transcriptome dynamics following FSH decline in bovine granulosa cells. *Biol Reprod* 2018; **99**:877–887.
3. Conti M, Franciosi F. Acquisition of oocyte competence to develop as an embryo: integrated nuclear and cytoplasmic events. *Hum Reprod Update* 2018; **24**:245–266.
4. Labrecque R, Sirard M-A. The study of mammalian oocyte competence by transcriptome analysis: progress and challenges. *Mol Hum Reprod* 2014; **20**:103–116.
5. Lazzaro MA, Pépin D, Pescador N, Murphy BD, Vanderhyden BC, Picketts DJ. The imitation switch protein SNF2L regulates steroidogenic acute regulatory protein expression during terminal differentiation of ovarian granulosa cells. *Mol Endocrinol* 2006; **20**:2406–2417.
6. Pépin D, Vanderhyden BC, Picketts DJ, Murphy BD. ISWI chromatin remodeling in ovarian somatic and germ cells: revenge of the NURFs. *Trends Endocrinol Metab* 2007; **18**:215–224.
7. Pépin D, Paradis F, Perez-Iratxeta C, Picketts DJ, Vanderhyden BC. The imitation switch ATPase Snf2l is required for superovulation and regulates Fgl2 in differentiating mouse granulosa cells. *Biol Reprod* 2013; **88**:142.
8. Bultman SJ, Gebuhr TC, Pan H, Svoboda P, Schultz RM, Magnuson T. Maternal BRG1 regulates zygotic genome activation in the mouse. *Genes Dev* 2006; **20**:1744–1754.
9. Trotter KW, Archer TK. The BRG1 transcriptional coregulator. *Nucl Recept Signal* 2008; **6**:e004.
10. Seneda MM, Godmann M, Murphy BD, Kimmins S, Bordignon V. Developmental regulation of histone H3 methylation at lysine 4 in the porcine ovary. *Reproduction* 2008; **135**:829–838.
11. Hans F, Dimitrov S. Histone H3 phosphorylation and cell division. *Oncogene* 2001; **20**:3021–3027.
12. Ruiz-Cortés ZT, Kimmins S, Monaco L, Burns KH, Sassone-Corsi P, Murphy BD. Estrogen mediates phosphorylation of histone H3 in ovarian follicle and mammary epithelial tumor cells via the mitotic kinase. *Aurora B Mol Endocrinol* 2005; **19**:2991–3000.
13. Singh AP, Foley JF, Rubino M, Boyle MC, Tandon A, Shah R, Archer TK. Brg1 enables rapid growth of the early embryo by suppressing genes that regulate apoptosis and cell growth arrest. *Mol Cell Biol* 2016; **36**:1990–2010.
14. Lisboa LA, Bordignon V, Seneda MM. Immunolocalization of BRG1-SWI/SNF protein during folliculogenesis in the porcine ovary. *Zygote* 2012; **20**:243–248.
15. Hendricks KB, Shanahan F, Lees E. Role for BRG1 in cell cycle control and tumor suppression. *Mol Cell Biol* 2004; **24**:362–376.
16. Sumi-Ichinose C, Ichinose H, Metzger D, Chambon P. SNF2beta-BRG1 is essential for the viability of F9 murine embryonal carcinoma cells. *Mol Cell Biol* 1997; **17**:5976–5986.
17. Reyes JC, Barra J, Muchardt C, Camus A, Babinet C, Yaniv M. Altered control of cellular proliferation in the absence of mammalian brahma (SNF2alpha). *EMBO J* 1998; **17**:6979–6991.
18. Jamin SP, Arango NA, Mishina Y, Hanks MC, Behringer RR. Requirement of Bmpr1a for Müllerian duct regression during male sexual development. *Nat Genet* 2002; **32**:408–410.
19. Fan H-Y, Shimada M, Liu Z, Cahill N, Noma N, Wu Y, Gossen J, Richards JS. Selective expression of KrasG12D in granulosa cells of the mouse ovary causes defects in follicle development and ovulation. *Development* 2008; **135**:2127–2137.
20. Lan Z-J, Xu X, Cooney AJ. Differential oocyte-specific expression of Cre recombinase activity in GDF-9-iCre, Zp3cre, and Msx2Cre transgenic mice. *Biol Reprod* 2004; **71**:1469–1474.
21. Pedersen T, Peters H. Proposal for a classification of oocytes and follicles in the mouse ovary. *J Reprod Fertil* 1968; **17**:555–557.
22. Boyer A, Lapointe É, Zheng X, Cowan RG, Li H, Quirk SM, Demayo FJ, Richards JS, Boerboom D. WNT4 is required for normal ovarian follicle development and female fertility. *FASEB J* 2010; **24**:3010–3025.
23. Stritt M, Stalder AK, Vezzali E. Orbit image analysis: an open-source whole slide image analysis tool. *PLoS Comput Biol* 2020; **16**:e1007313.
24. Zhang Y, Yan Z, Qin Q, Nisenblat V, Chang H-M, Yu Y, Wang T, Lu C, Yang M, Yang S, Yao Y, Zhu X *et al.* Transcriptome landscape of human Folliculogenesis reveals oocyte and granulosa cell interactions. *Mol Cell* 2018; **72**:1021–1034.e4.
25. Khan DR, Fournier É, Dufort I, Richard FJ, Singh J, Sirard M-A. Meta-analysis of gene expression profiles in granulosa cells during folliculogenesis. *Reproduction* 2016; **151**:R103–R110.
26. Robert C, Nieminen J, Dufort I, Gagné D, Grant JR, Cagnone G, Plourde D, Nivet A-L, Fournier É, Paquet É, Blazejczyk M, Rigault P *et al.* Combining resources to obtain a comprehensive survey of the bovine embryo transcriptome through deep sequencing and microarrays. *Mol Reprod Dev* 2011; **78**:651–664.
27. Cuthbert JM, Russell SJ, White KL, Benninghoff AD. The maternal-to-zygotic transition in bovine in vitro-fertilized embryos is associated with marked changes in small non-coding RNAs†. *Biol Reprod* 2019; **100**:331–350.
28. Hernandez Gifford JA, Hunzicker-Dunn ME, Nilson JH. Conditional deletion of beta-catenin mediated by Amhr2cre in mice causes female infertility. *Biol Reprod* 2009; **80**:1282–1292.
29. Fan H-Y, Liu Z, Paquet M, Wang J, Lydon JP, DeMayo FJ, Richards JS. Cell type-specific targeted mutations of Kras and Pten document proliferation arrest in granulosa cells versus oncogenic insult to ovarian surface epithelial cells. *Cancer Res* 2009; **69**: 6463–6472.
30. Blondin P, Coenen K, Guilbault LA, Sirard MA. Superovulation can reduce the developmental competence of bovine embryos. *Theriogenology* 1996; **46**:1191–1203.
31. Attanasio C, Nord AS, Zhu Y, Blow MJ, Biddie SC, Mendenhall EM, Dixon J, Wright C, Hosseini R, Akiyama JA, Holt A, Plajzer-Frick I *et al.* Tissue-specific SMARCA4 binding at active and repressed regulatory elements during embryogenesis. *Genome Res* 2014; **24**:920–929.
32. Bultman S, Gebuhr T, Yee D, La Mantia C, Nicholson J, Gilliam A, Randazzo F, Metzger D, Chambon P, Crabtree G, Magnuson T. A Brg1 null mutation in the mouse reveals functional differences among mammalian SWI/SNF complexes. *Mol Cell* 2000; **6**: 1287–1295.
33. Pangas SA, Choi Y, Ballow DJ, Zhao Y, Westphal H, Matzuk MM, Rajkovic A. Oogenesis requires germ cell-specific transcriptional regulators Sohlh1 and Lhx8. *Proc Natl Acad Sci U S A* 2006; **103**: 8090–8095.
34. Edson MA, Nagaraja AK, Matzuk MM. The mammalian ovary from genesis to revelation. *Endocr Rev* 2009; **30**:624–712.
35. Reisman DN, Sciarrotta J, Bouldin TW, Weissman BE, Funkhouser WK. The expression of the SWI/SNF ATPase subunits BRG1 and BRM in normal human tissues. *Appl Immunohistochem Mol Morphol* 2005; **13**:66–74.

36. Savas S, Skardasi G. The SWI/SNF complex subunit genes: their functions, variations, and links to risk and survival outcomes in human cancers. *Crit Rev Oncol Hematol* 2018; **123**: 114–131.
37. Sobczak M, Pietrzak J, Płoszaj T, Robaszkiewicz A. BRG1 activates proliferation and transcription of cell cycle-dependent genes in breast cancer cells. *Cancers* 2020; **12**:12.
38. Wang B, Kaufmann B, Engleitner T, Lu M, Mogler C, Olsavszky V, Öllinger R, Zhong S, Geraud C, Cheng Z, Rad RR, Schmid RM *et al.* Brg1 promotes liver regeneration after partial hepatectomy via regulation of cell cycle. *Sci Rep* 2019; **9**: 2320.
39. Trouche D, Le Chalony C, Muchardt C, Yaniv M, Kouzarides T. RB and hbrm cooperate to repress the activation functions of E2F1. *Proc Natl Acad Sci U S A* 1997; **94**:11268–11273.
40. Uchida C. Roles of pRB in the regulation of nucleosome and chromatin structures. *Biomed Res Int* 2016; **2016**:5959721.
41. Giacinti C, Giordano A. RB and cell cycle progression. *Oncogene* 2006; **25**:5220–5227.
42. Kothandapani A, Gopalakrishnan K, Kahali B, Reisman D, Patrick SM. Downregulation of SWI/SNF chromatin remodeling factor subunits modulates cisplatin cytotoxicity. *Exp Cell Res* 2012; **318**: 1973–1986.
43. Combelles CMH, Albertini DF. Assessment of oocyte quality following repeated gonadotropin stimulation in the mouse. *Biol Reprod* 2003; **68**:812–821.
44. Apolloni LB, Bruno JB, Alves BG, Ferreira ACA, Paes VM, de Moreno J, FLN DA, Brandão FZ, Smitz J, Apgar G, De Figueiredo JR. Accelerated follicle growth during the culture of isolated caprine preantral follicles is detrimental to follicular survival and oocyte meiotic resumption. *Theriogenology* 2016; **86**: 1530–1540.
45. Cadoret V, Frapsauce C, Jarrier P, Maillard V, Bonnet A, Locatelli Y, Royère D, Monniaux D, Guérif F, Monget P. Molecular evidence that follicle development is accelerated in vitro compared to in vivo. *Reproduction* 2017; **153**:493–508.
46. Eppig JJ, O'Brien MJ, Pendola FL, Watanabe S. Factors affecting the developmental competence of mouse oocytes grown in vitro: follicle-stimulating hormone and insulin. *Biol Reprod* 1998; **59**: 1445–1453.
47. Tan J-H, Wang H-L, Sun X-S, Liu Y, Sui H-S, Zhang J. Chromatin configurations in the germinal vesicle of mammalian oocytes. *Mol Hum Reprod* 2009; **15**:1–9.
48. Zuccotti M, Piccinelli A, Giorgi Rossi P, Garagna S, Redi CA. Chromatin organization during mouse oocyte growth. *Mol Reprod Dev* 1995; **41**:479–485.
49. Bourgo RJ, Siddiqui H, Fox S, Solomon D, Sansam CG, Yaniv M, Muchardt C, Metzger D, Chambon P, Roberts CWM, Knudsen ES. SWI/SNF deficiency results in aberrant chromatin organization, mitotic failure, and diminished proliferative capacity. *Mol Biol Cell* 2009; **20**:3192–3199.
50. Sethy R, Rakesh R, Patne K, Arya V, Sharma T, Haokip DT, Kumari R, Muthuswami R. Regulation of ATM and ATR by SMARCAL1 and BRG1. *Biochim Biophys Acta Gene Regul Mech* 2018; **1861**:1076–1092.
51. Baumann C, Viveiros MM, De La Fuente R. Loss of maternal ATRX results in centromere instability and aneuploidy in the mammalian oocyte and pre-implantation embryo. *PLoS Genet* 2010; **6**:e1001137.
52. Young RH, Oliva E, Scully RE. Small cell carcinoma of the ovary, hypercalcemic type. A clinicopathological analysis of 150 cases. *Am J Surg Pathol* 1994; **18**:1102–1116.
53. Gamwell LF, Gambaro K, Merziotis M, Crane C, Arcand SL, Bourada V, Davis C, Squire JA, Huntsman DG, Tonin PN, Vanderhyden BC. Small cell ovarian carcinoma: genomic stability and responsiveness to therapeutics. *Orphanet J Rare Dis* 2013; **8**:33.
54. Kupryjańczyk J, Dansonka-Mieszkowska A, Moes-Sosnowska J, Plisiecka-Hałasa J, Szafron L, Podgórska A, Rzepecka IK, Konopka B, Budziłowska A, Rembiszewska A, Grajkowska W, Spiewankiewicz B. Ovarian small cell carcinoma of hypercalcemic type - evidence of germline origin and SMARCA4 gene inactivation. A pilot study. *Pol J Pathol* 2013; **64**:238–246.
55. Witkowski L, Carrot-Zhang J, Albrecht S, Fahiminiya S, Hamel N, Tomiak E, Grynspan D, Saloustros E, Nadaf J, Rivera B, Gilpin C, Castellsagué E *et al.* Germline and somatic SMARCA4 mutations characterize small cell carcinoma of the ovary, hypercalcemic type. *Nat Genet* 2014; **46**:438–443.
56. Ramos P, Karnezis AN, Craig DW, Sekulic A, Russell ML, Hendricks WPD, Corneveaux JJ, Barrett MT, Shumansky K, Yang Y, Shah SP, Prentice LM *et al.* Small cell carcinoma of the ovary, hypercalcemic type, displays frequent inactivating germline and somatic mutations in SMARCA4. *Nat Genet* 2014; **46**:427–429.
57. Jelinic P, Mueller JJ, Olvera N, Dao F, Scott SN, Shah R, Gao J, Schultz N, Gonen M, Soslow RA, Berger MF, Levine DA. Recurrent SMARCA4 mutations in small cell carcinoma of the ovary. *Nat Genet* 2014; **46**:424–426.